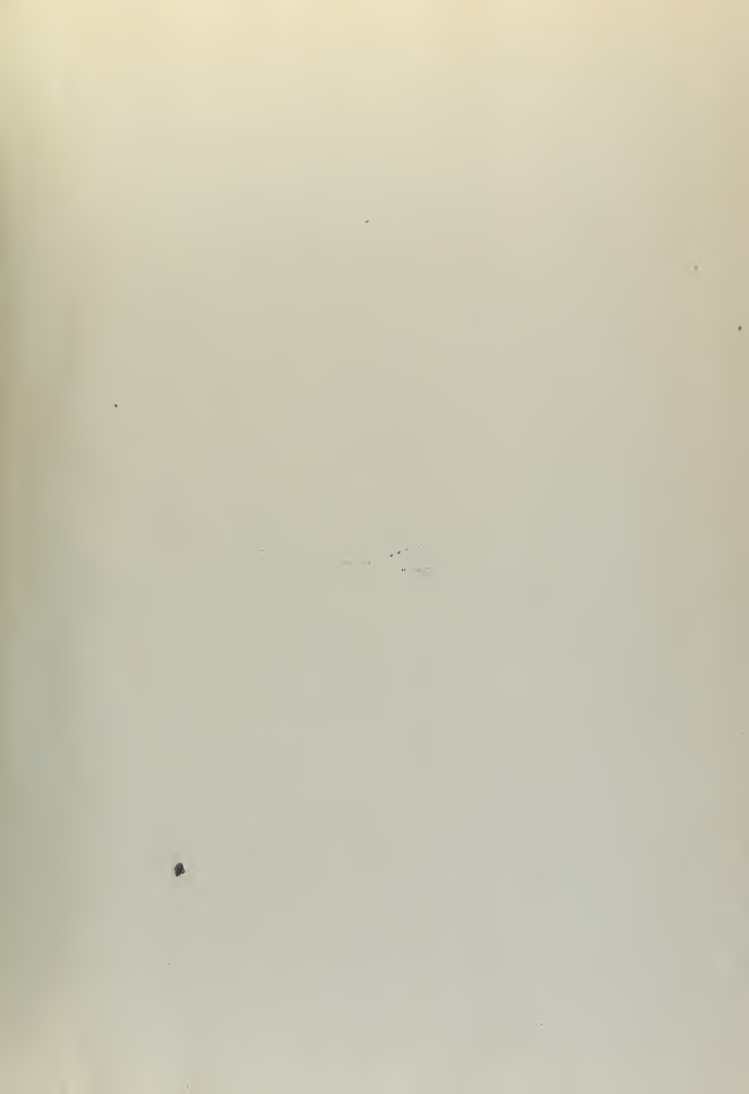


AN INVESTIGATION OF THE FORMATION
OF PLASTIC HINGES IN SIMPLE
RIGID FRAMES

WILLIAM E. MONAGHAN AND
THOMAS C. WILLIAMS

29W
THESES

Library
U. S. Naval Postgraduate School
Monterey, California





AN INVESTIGATION
of the
FORMATION OF PLASTIC HINGES
in
SIMPLE RIGID FRAMES

By
William E. Monaghan
" "
and
Thomas C. Williams

Submitted to
The Faculty of Rensselaer Polytechnic Institute
in partial fulfillment of the requirements for
the degree of
Master of Civil Engineering

June, 1951
Troy, New York

ACKNOWLEDGEMENTS

The authors wish to express their appreciation for the assistance and advice given them by Professor R. H. Trathen throughout this investigation.

We also wish to thank Professor J. F. Throop and Doctor Ernest F. Nippes of the Metallurgy Department for furnishing some of the equipment necessary in the conduct of our thesis.

TABLE OF CONTENTS

	<u>Page</u>
INTRODUCTION	
Object	1
Scope	2
THEORY	
Preliminary	3
Basic Considerations.	3
Figures 1 and 2	4
Limit Design.	5
Plastic Hinge and Plastic Moment.	7
Figure 3.	8
Extent of Ductile Flow.	9
Redundant Structures.	10
Figure 4.	11
Admissibility of Assumed Plastic Hinges	12
Practical Procedure for Testing Assumed Hinges	13
Figure 5.	14
Figure 6.	17
TESTING APPARATUS	
Test Bench.	18
Figure 7.	19
Knife-Edge Supports	20
Load Applicators.	20
Figure 8-A.	21
Test Weights.	22
Deflection Gages.	22
Rigid Frame Holder.	22
Figure 8-B.	23
Base Plate and Clamps	24
Comments.	24
Photographs	25
METHOD OF TESTING	
Test Samples.	26
Figure 9.	27
Preliminary	29
Applying Loads.	30
Determining Plastic Hinge Formation.	30

TABLE OF CONTENTS (Cont'd)

Page

RESULTS AND DISCUSSION

Tensile Tests	32
Simple Beam Tests	32
Frame Tests #1, #2, and #3	33
Figure 10-A	34
Figure 10-B	36
Frame Tests #4, #5, and #6	37
Photographs for Frame Tests #1-#6	38
Figure 11	40
Frame Tests #7, #8, and #9	41
Figure 12-A	42
Figure 12-B	44
Photographs for Frame Tests #7-#12	45
Frame Tests #10, #11, and #12	46
Figure 13-A	47
Figure 13-B	49
Frame Tests #13, #14, and #15	52
Figure 14	53
Photographs for Frame Tests #13-#18	54
Frame Tests #16, #17, and #18	55
Figure 15	56
Frame Tests #19 and #20	57
Figure 16	58
Photographs	60
Theoretical Analysis of Two-Bay Single Story Rigid Frame	61
Figure 17	62
CONCLUSIONS	63
RECOMMENDATIONS	65
APPENDIX	66

INTRODUCTION

Object:

The objects of this thesis are two-fold: First, to outline a simplified method for limit design of simple rigid frames. Second, to attempt to verify by experimental results that the theoretical design procedure gives a reasonably accurate picture of the true strength of the various frames tested.

The theoretical principles involved in the procedures of limit design have been set forth in detail by J. A. VAN DEN BROEK in his book entitled, "Theory of Limit Design", and by H. J. GREENBERG and W. PRAGER from Brown University in their technical report entitled "Limit Design of Beams and Frames".

This thesis is an extension of the thesis, presented to the Faculty of Rensselaer Polytechnic Institute, by Charles W. BUTLER and James I. GIBSON entitled, "An Investigation of the Formation of Plastic Hinges in Simple Structures".

Scope:

It was felt that in this investigation it was more important to conduct experiments using a single concentrated load on a number of different types of simple rigid frames rather than subjecting a few test models to a great variety of loading conditions. Furthermore, since we felt that the ability to predict the absolute value of the plastic moment was incidental to the ability to predict the loads required to form plastic hinges, we decided to use models with rectangular cross sections in the interests of simplicity and economy. The test apparatus used by Butler and Gibson in the conduct of their thesis work proved satisfactory for our work. It was necessary to modify their equipment slightly in order that we might test frames with legs of unequal length.

THEORY

Preliminary:

As applied to statically indeterminate structures, the method of limit design is based upon the assumption that the relationship between the stress and strain at any point in the material of a structure is as shown in Figure 1.

The distance BC in Figure 1 represents yielding under constant load and is from 10 to 20 times the distance A'B. The distance A"D is from 200 to 300 times as large as A'B.

It is essential that the material used in structures designed by limit design procedure exhibit this property of ductility (excessive deformation under substantially constant load). In this thesis, ductility will refer to the property of the material by virtue of which ductile flow is able to take place. Plasticity will refer to the ductile behavior of a structural member in a region where complete ductile flow has occurred.

Basic Considerations:

Any theory is based upon assumptions or premises. The theory of strength is predicated on two basic considerations: First, that of equilibrium; and second, that of continuity. The first is by far the more important of the two. It is expressed conventionally in two dimensional analysis by:

$$\leq F_x = 0 \quad \leq F_y = 0 \quad \leq M = 0$$

FIGURE 1

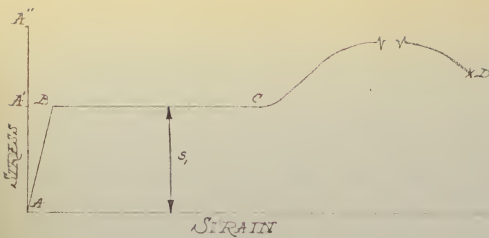
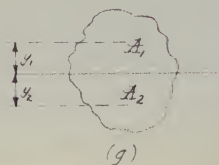
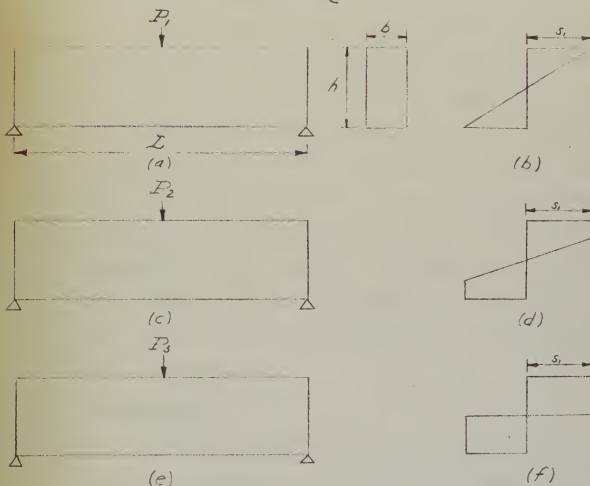


FIGURE 2



Any violation of the laws of equilibrium, no matter how minor, results in collapse. The conditions of continuity are secondary to those of static equilibrium and serve to supplement the latter in arriving at a picture of the strength of a given structure. To satisfy the conditions of continuity, we have the choice of two theories. One presupposes elastic behavior and elastic stress distribution, while the other presupposes ductile stress distribution. The former is known as the "theory of elasticity" and the latter as the "theory of limit design".

The theory of elasticity argues that the primary criterion of strength is the elastic working stress. The theory of limit design argues that the primary criterion of strength is deformation. The theory of elasticity is well known to all structural engineers and needs no review. The theory of limit design is less familiar and so a description of its application will be presented.

Limit Design:

The application of the theory of limit design can best be shown by considering the simple beam in Figure 2-A with a concentrated load at the mid-point. The maximum value of the load P for which the elastic-limit stress, s_1 , is just reached in the outer fibers under the load is found from the equation,

$$s_1 = Mc/I = 3P_1 L/2 bh^2$$

from which $P_1 = 2s_1bh^2/3L$. The stress distribution over the cross-section of the beam will then be as shown in Figure 2-b. If the elastic-ductile properties of the material correspond to curve ABC in Figure 1; further, if a plane before bending remains a plane after bending in any elastic part of the beam, then the stress distribution under the load P_2 (Figure 2-c), slightly in excess of P_1 will be as shown in Figure 2-d. The limiting resisting moment of the beam will be developed when all of the fibers over the entire cross-section are stressed with their elastic limit stress s_1 . The stress distribution under the load P_3 (Figure 2-e) will be as shown in Figure 2-f. Let Figure 2-g represent the cross-section on which this limit stress distribution has been reached. From $\sum F_x = 0$ we derive $A_1s_1 = A_2s_1$ and hence $A_1 = A_2$. Thus it will be seen that in an unsymmetrical beam, the neutral axis does not necessarily pass through the centroid of the cross section. The bending moment resulting from the stress distribution of Figure 2-f would be: $M = s_1(A_1y_1 + A_2y_2)$. In the case of a symmetrical beam, the neutral axis passes through the centroid of the section and $A_1y_1 = A_2y_2$. In this case $M = 2s_1\bar{Ay}$ where \bar{Ay} represents the static moment about the neutral axis of that part of the cross-sectional area which lies to one side of the neutral axis. Thus for the rectangular section in

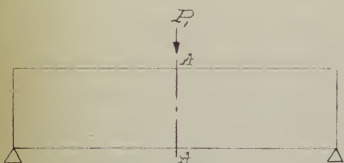
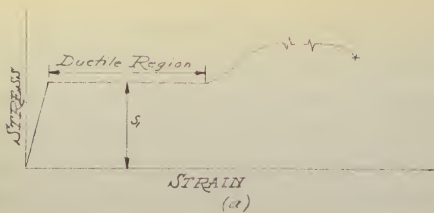
Figure 2-a, $M = 2s_1(bh/2)(h/4) = s_1bh^2/4$ and $P_3 = s_1bh^2/L$. Thus the limit load carrying capacity of a simple rectangular beam is 50% greater than it's elastic load carrying capacity.

Plastic Hinge and Plastic Moment:

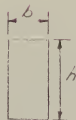
Plastic hinges are a property of a point or points in a structure by virtue of which extensive bending occurs at the point or points under a constant or slightly increasing bending moment. The steps in the formation of a plastic hinge are illustrated in Figure 3.

Figure 3-a shows the idealized stress-strain curve for mild steel for purposes of reference. Consider the beam in Figure 3-b loaded with a concentrated load at mid-span equal to P_1 (Figure 3-b) which stresses the extreme fiber in the beam at section A-A up to the elastic limit s_1 , (Figure 3-c). The moment existing under load P_1 is equal to $s_1bh^2/6$. If the elastic limit in the top and bottom fibers of the beam in the vicinity of section A-A is exceeded by increasing load P_1 to a value P_2 (Figure 3-d), then the stress distribution over the cross section of the beam appears as shown in Figure 3-e and the magnitude of the moment existing under the load P_2 is expressed as $M_2 = s_1b(h^2/4 - y^2/3)$.

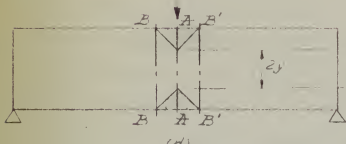
FIGURE 3



(b)



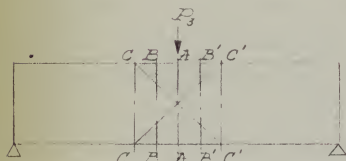
(c)



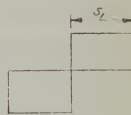
(d)



(e)



(f)



(g)

When load P_3 (Figure 3-f) is applied so that all of the fibers over the entire cross-section A-A have become ductile (Figure 3-g), then y in the previous equation equals zero and we obtain $M_3 = s_1 b h^2 / 4$ which is merely the formula $M = 2s_1 A \cdot \bar{y}$ for a rectangular section, in which M_3 is defined as the plastic moment for section A-A. Since all fibers of section A-A in the beam shown in Figure 3-f are now in the ductile region of the stress-strain curve of Figure 3-a, the beam will bend extensively at section A-A under the constant load P_3 . Thus section A-A may be called a plastic hinge and the moment M_3 existing at section A-A may be called the plastic moment for the section.

Extent of Ductile Flow:

The shaded portions of Figures 3-d and 3-f represent the area of the beam in which ductile flow has occurred. Beyond the area of ductile flow, normal elastic behavior exists in every respect. Thus at section B-B and B'-B' in Figure 3-d, the stress pattern is as shown in Figure 3-c. Similarly, at section C-C and C'-C' in Figure 3-f, the stress pattern is also as shown in Figure 3-c, while at sections B-B and B'-B' in Figure 3-f, the stress pattern is as shown in Figure 3-e. The area of depth $2y$, as shown in Figure 3-d, between the zones of ductile flow, is referred to herein as the elastic core. The existence of this

elastic core means that the beam will act elastically under any moment less than the plastic moment. This means that up until the time that the plastic hinge forms, the deflections will be elastic deflections, and that the plot of load versus deflections should be of constant slope right out to the point where the hinge has completely formed.

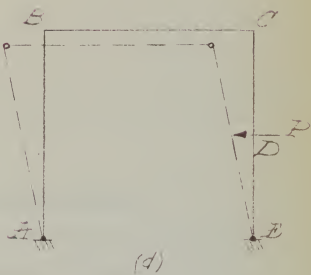
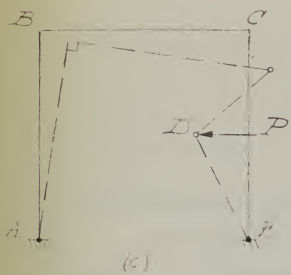
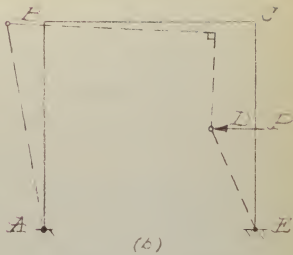
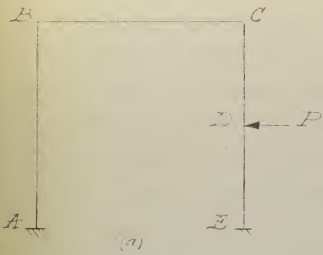
Redundant Structures:

For a detailed discussion of the theory of limit design as applied to fixed-end and continuous beams the readers of this thesis are referred to the Butler-Gibson thesis previously referenced. In this thesis we have attempted only to discuss the application of the theory of limit design as applied to simple rigid frames.

In the discussion that follows, the term "mechanism" appears and will be defined here:

A structure becomes a mechanism when plastic hinges form in sufficient number such that, despite the assumed rigidity of its members, the structure is capable of at least an infinitesimal deformation. To test whether or not a mechanism exists, it is only necessary to replace the plastic hinges by real hinges and see if deformation can take place under the given loading. For instance, the frame in Figure 4-a becomes a mechanism if plastic hinges develop at points A, B, D, E, Figure 4-b;

FIGURE 4



A, C, D, E, Figure 4-c; or A, B, C, E, Figure 4-d.

The frame is then capable of the deformations indicated by the dotted lines. The reader will naturally wonder how many hinges must develop in a given structure in order for a mechanism to form. The following axiom can be applied to determine the necessary number:

"In a structure that is n -fold redundant, it is necessary and sufficient that ($n-1$) plastic hinges be formed in order that the structure be transformed into a mechanism".

The reason behind this axiom is simply that the insertion of ($n-1$) hinges reduces the number of reactions to one less than that required for stable equilibrium, and hence the structure collapses. Thus the frame in Figure 4-a being three-fold redundant requires that four plastic hinges form in order to become a mechanism.

Admissibility of Assumed Plastic Hinges:

The following rule is proposed as a basis and criterion for testing redundant structures for the validity of assumed plastic hinges: "Assume the plastic moment to exist at the points of assumed plastic hinges in the structure, provided such assumptions are in accordance with the equations of equilibrium, and solve for the load or loads which are statically

compatible with the assumed values of plastic moments.

Draw the bending moment diagram for the structure.

If at each point in the structure the absolute value of the bending moment does not exceed the value of the plastic moment that can exist at that section, then the plastic hinges that have been assumed are said to be statically admissible. The sense of the plastic moments follows from the sense of the relative rotations of the members of the structure which occur when the structure acts as a mechanism. The direction of the plastic moment acting on a member tends to oppose the rotation of that member.

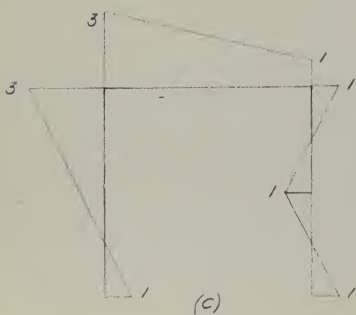
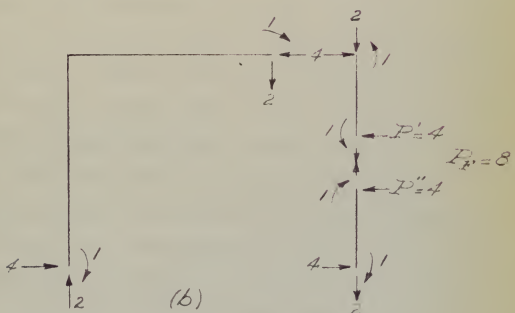
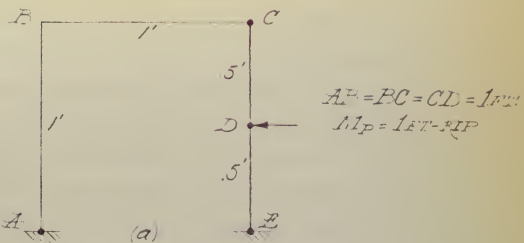
Practical Procedure for Testing Assumed Hinges:

In this section we will show the procedure to be followed in the analysis of a typical simple rigid frame.

Location of plastic hinges incorrectly assumed:

In Figure 5-a, plastic hinges have been assumed to form at A, D, E, and C. Since the cross-sectional area is constant throughout this frame, we have assumed a value of 1 foot-kip for the plastic moment. Free bodies are drawn for the sections of the frame between assumed plastic hinges. Solutions of these free bodies by the formulas of statics gives us the values of

FIGURE 5



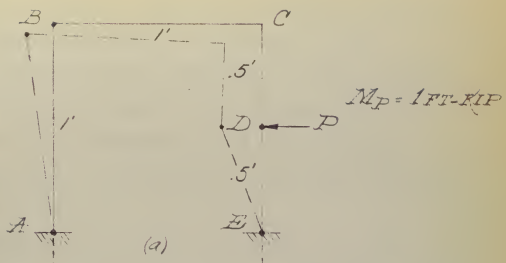
redundant reactions and the force P , shown in Figure 5-b. A check of the free bodies and of the structure as a whole, shows that the loads and redundant reactions are externally statically admissible. It is now necessary to determine that the plastic moment is not exceeded at any point in the structure. All of the data for constructing a bending moment diagram is available. In drawing the bending moment diagram it is seen that the moment at B under the action of the load and redundants shown is equal to 3 foot-kips. Although such a moment is obviously impossible in a structure whose plastic moment is only 1 foot-kip, the bending moment diagram is plotted in Figure 5-c to show how it violates the proposed rule. Since the bending moment at B exceeds the plastic moment, it is obvious that the locations of the plastic hinges have been incorrectly assumed and that 8 kips is not a valid value of the failure load.

Location of plastic hinges correctly assumed:

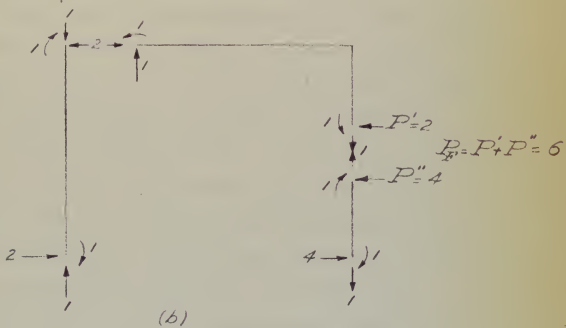
It might be well to note at this point that certain rules can be followed in locating some of the hinges. The first hinge will always form at the point of maximum elastic bending moment. The other hinges must be located according to one's logic. If the first assumption of hinges is incorrect, (i.e., if the moment at any point or points in the frame exceeds the plastic moment) then a hinge, or hinges, should be assumed at the point, or points, where the plastic moment was exceeded for the next analysis.

Now let us take the same frame and assume plastic hinges at A, B, D, and E (Figure 6-a). The frame is now broken up into free bodies of the sections between plastic hinges and a solution is made for the redundant reactions and the load P by statics (Figure 6-b). The bending moment diagram for the frame is drawn in Figure 6-c. At no point in the frame does the value of the bending moment exceed the corresponding value of the plastic moment. Therefore, the locations of the plastic hinges have been correctly assumed and the value of the load P is the correct value of the failure load.

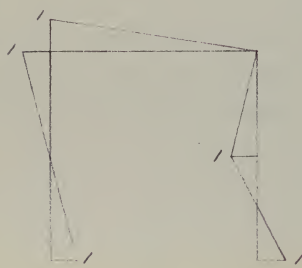
FIGURE 6



(a)



(b)



(c)

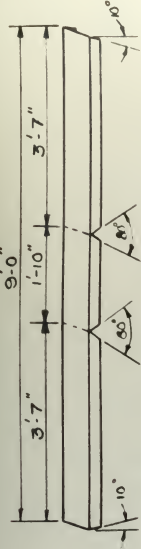
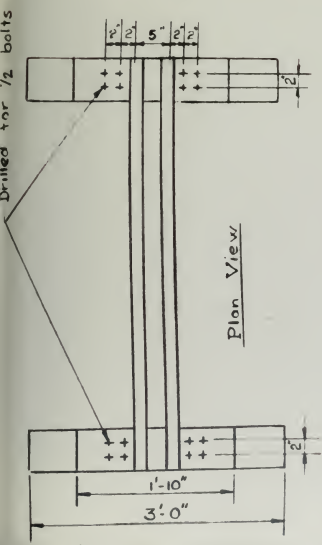
TESTING APPARATUS

After looking up sufficient background material pertaining to the scope of our thesis, it was decided that with minor modifications, the equipment used by Butler and Gibson in the conduct of their thesis would be satisfactory for our laboratory investigations. A description of the test equipment follows:

Test Bench:

The main part of the apparatus was the test bench which was of very sturdy design in order to assure that there would be no deflection of the bench itself caused by the loading of the model. The bench was made, as the accompanying Figure 7 shows, of 6-inch channels. Two nine foot lengths were bent to form the legs of the bench and two five foot lengths were bolted on to the flat tops of these supports to form the cross members for support of the knife edges which were used to support beam models, as well as to support the base plates for testing rigid frames. The cross member channels were placed with their flanges outward so that these flanges could be utilized for clamping on the deflection gages.

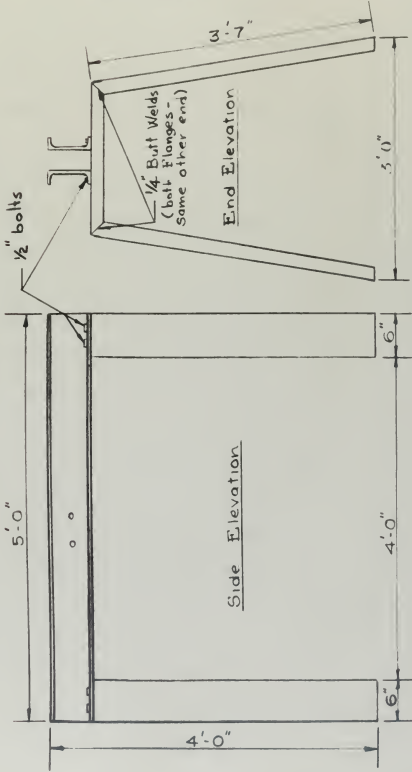
FIGURE



TEST BENCH DETAIL

Scale ~ $\frac{3}{4}'' = 1'-0''$

Note: All parts are fabricated from 6" L 8.2 sections.



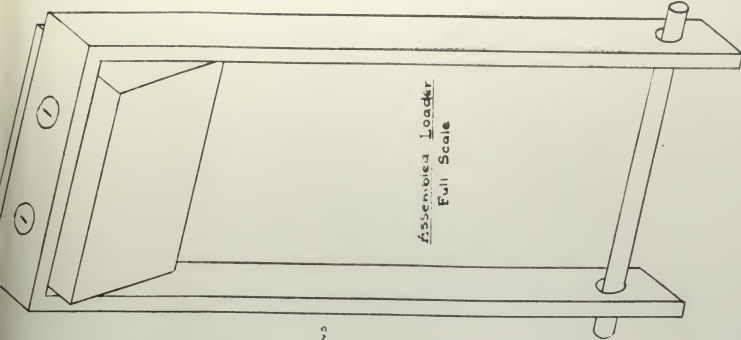
Knife-edge Supports:

The knife-edges used to support the simple beam models which were used in determining the value of yield stresses for the materials used were machined down to form a sharp knife-edged support. The bottoms were rounded in order to allow the support to rotate as the loads were applied to the beam. The idea behind this was to keep the reaction vertical. The knife edges were made long enough to give good bearing on the cross member channels. (See Figure 8-A)

Load Applicators:

Hangers were used for applying the load to the frames tested. This allowed the load to be applied to the top of the members while adding the weights below the bench, thus facilitating the loading procedure. The load applicator itself was a machined knife-edge which had a strap bent over the top of it in the shape of an inverted U. The strap was bolted to the knife-edge. Through the ends of the legs of the inverted U, holes were drilled, through which a round pin was inserted. (See Figure 8-A). A rod hooked on both ends was hung over this round pin. The bottom hook was used to support the bucket in which loads were placed.

FIGURE 8A.



Assembly Loader
Full Scale

卷之三

Detector at Krater-eair:
Scale: $\frac{1}{2}''$ | support:
Make A

1044 *Int. J. Environ. Res. Public Health* 2020, 17, 1044

1 and Tap for 1/4 machine Screws

sides machine

Detail for Louder and Hanger
Scale ~ $\frac{1}{2}$ " = 1' 0"

Test Weights:

Twenty-five pound bags of lead shot; cast iron ingots weighing approximately 8 pounds; and small lead pellets weighing four-tenths of a pound each were used as weights. Each of the weights used was weighed and its weight to the nearest tenth of a pound was determined and recorded.

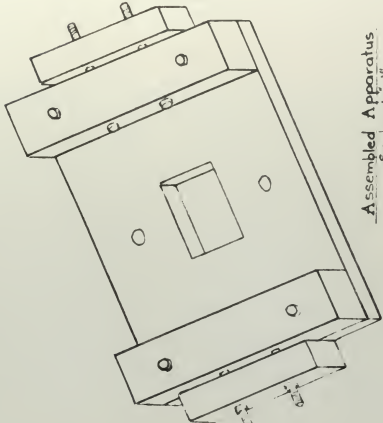
Deflection Gages:

Deflection gages were used primarily as an aid in observing when the formation of the plastic hinges occurred. That is, upon the formation of each hinge there was an abnormally large change in dial reading. The dial holders were clamped by means of small C-clamps to the flanges of the cross members. The linkages of the holders gave versatility to the use of the gages as they could be adjusted to any position for taking readings as necessary.

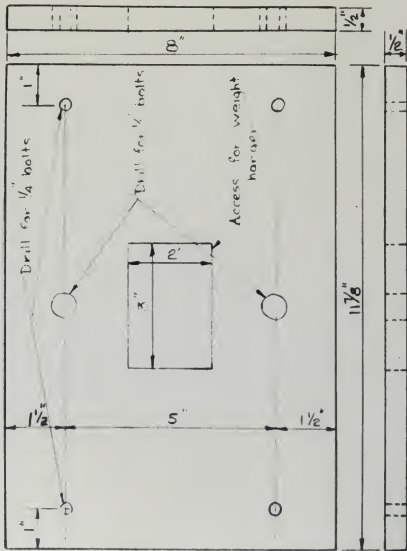
Rigid Frame Holder:

This holder was designed to accommodate a frame span width of one foot. The value of one foot was chosen to simplify calculations. The frame leg clamps were designed to give a rigid connection. (See Figure 8-B).

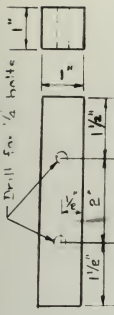
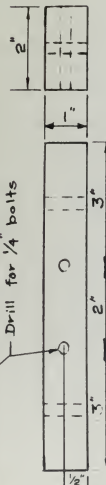
FIGURE 8B



RIGID FRAME TESTER
Scale ~ $\frac{3}{8}'' = 1''$

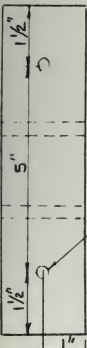


Exterior Shape



Front View

Drill for $\frac{1}{4}$ " bolts



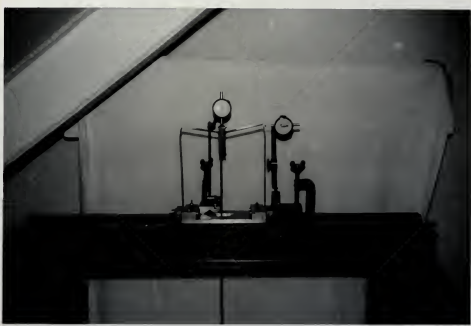
Drill for $\frac{1}{4}$ " bolts

Base Plate and Clamps:

The base plate and clamp blocks were machined to give as smooth a bearing surface as possible. The base plate was drilled with holes for $\frac{1}{2}$ " bolts so that it could be bolted to the side of the main testing bench in such a way as to allow the simulation of a side load on the leg of the frame. A hole was cut in the center of the base plate to allow for the suspension of the test weights when simulating a vertical load on the horizontal top member of the frame. In order to test frames with unequal legs, it was necessary to build up one set of clamping blocks. For facilitating computations, a built-up height of one-half foot was chosen.

Comments:

For our investigations, the apparatus proved satisfactory. However, for more complicated loading schemes and for the analysis of more complicated structures, the equipment would necessarily have to be modified. Pictures relative to equipment described in this section are included on the next page.





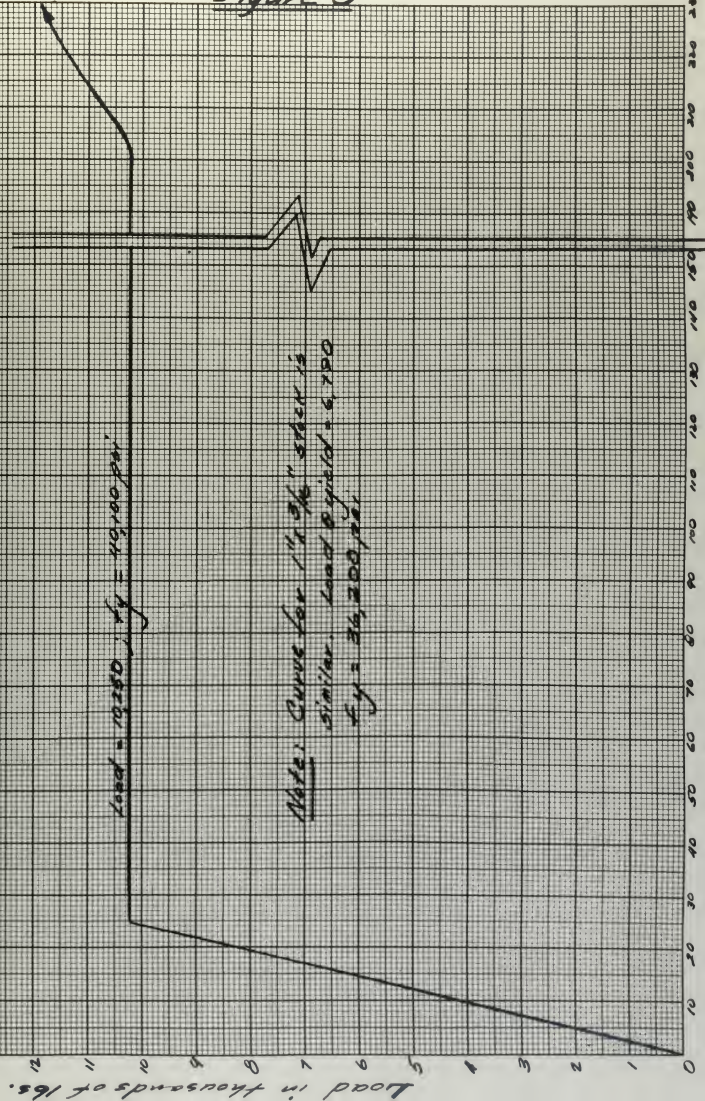
METHOD OF TESTING

In order to calculate predicted failure loads, it was necessary to determine the yield strength of the materials used. A simple beam test provided the most direct and simple method for determining the yield strengths of the materials. As a check on the value of the yield stress determined by developing the plastic moment in a simple beam test, tensile test specimens were made up and tested in a Riehle Testing Machine in the Mechanics Laboratory. Since the test models were fabricated from two types of steel, two sets of tensile tests were necessary. A stress-strain curve for each of the two tests is included in Figure 9. Each of the curves shows that the material exhibits the required ductility for the application of limit design. The simple beam tests were considered to be more accurate indications of the yield strengths, since they took into account the amount the cross section of the materials might have varied from the exact rectangular, which was the section assumed in the theoretical calculations.

Test Samples:

Two sizes of strap steel were used to fabricate the test models; 1" x 1/4" and 1" x 3/16". The strap steel was, in both cases, hot-rolled, mild steel.

Figure 9



The strap steel was bent hot to form the frames tested. The top member of each frame was made equal to one foot; the legs were made approximately one and one-half feet in order to obtain a good grip in the frame supports.

Since it was desired to test frames whose members were not all of the same moment of inertia, certain members of some of the frames were machined after the frames were bent. The inside angles at the corners were bent to a sharp 90 degrees.

The 3/16" strap was bent and all outside faces were machined so as to reduce the thickness of all portions of the frame to 1/8" which, in effect, reduced the magnitude of the failure loads to a reasonable value.

The 1/4" strap was bent and either the top member alone, or the two legs alone, were machined so as to reduce the thickness of the member or members to 1/8". This gave a cross sectional area ratio of 2 to 1 for the members.

In bending the strap steel to a sharp 90° inside corner, there was considerable reduction in cross sectional area at the corners. The machining operation helped to square-up the corners, thus minimizing the above effect.

The test specimens used in the determination of yield strengths by developing plastic moments in simple beam tests were cut from the same stocks as the frames. They were cut to lengths somewhat in excess of one foot so that a one foot span could be used, thus facilitating computations.

The yield strength of frames fabricated from the 3/16" stock was found to be 36,500 psi. The yield strength of frames made from the 1/4" stock was 40,300 psi.

Since it was not possible to have the frames heat-treated locally, we felt that the loss of time that would be involved in shipping the frames to be heat-treated was not warranted.

Preliminary:

Marks were scribed on each frame at the load point and points on each leg to give the proper leg length. The frame to be tested was placed in the supports and the frame leg clamps were bolted tightly. A load hanger was placed over the load point and a deflection gage was mounted with its plunger resting on the top of the hanger. In some cases a second gage was placed in a strategic location in order to observe lateral deflection of the leg.

Applying Loads:

The loading bucket was suspended from the hanger by means of a steel rod hooked at both ends. The heavy cast-iron ingots were used in loading until the theoretically calculated failure load was approached, at which time we switched to the .4# lead pellets. The individual and accumulated loads were noted and recorded as each additional weight was added. As the point in the loading near the formation of the plastic hinge at some section in the test structure was reached, the loading and observation of the deflection gages was carefully carried out. Extreme care had to be taken to make sure that the loading buckets were not allowed to swing back and forth in pendulum action, or to rock due to any vibration or other disturbance of the apparatus. In some test runs, it was found that this rocking tended to speed up the formation of the plastic hinges. The final load which transformed the structure into a mechanism is termed in this paper, "the failure load".

Determining Plastic Hinge Formation:

The following ways were used in determining when plastic hinges formed in the test structures: First, by observing the deflection gages. Whenever a hinge formed in the test structures, it was noted that the deflection gage reading increased considerably when compared to previous deflection increments. Secondly,

at the point or points at which a hinge or hinges formed, the elastic curve for the structure was no longer a smooth curve but rather exhibited a sharp bend, visible to the naked eye. Third, scaling of the material took place in the area of the plastic hinge. Last of all, as the hinge was forming, a "creaking" sound caused by the internal yielding of the material could be heard.

RESULTS AND DISCUSSION

Tensile Tests:

Curves of the tensile tests for the two types of strap steel used in our investigation are plotted in Figure 9. The values of the yield strengths of the two materials were found to be 36,200 psi. for the 1" x 3/16" stock and 40,100 psi. for the 1" x 1/4" stock. These values compare very closely with those obtained by simple beam tests.

Simple Beam Tests: (Load at mid-point of 12" span)

The yield strengths found from these tests were 36,500 psi. for the 1" x 3/16" stock and 40,300 psi. for the 1" x 1/4" stock. For reasons previously noted, these values were considered more valid than those obtained from the tensile tests on the specimens and consequently, were used in our theoretical calculations. The results of these tests together with results of all following tests are included in the appendix. These simple beam tests provided for us the first opportunity to observe the formation of a plastic hinge. As the load was applied to the beam, it deflected in the normal manner. This deflection curve existed until the instant that the plastic hinge formed under the load. At this time, the curvature completely disappeared, the sections on either side of the hinge becoming perfectly straight. It was necessary to relieve the load in order to stop the collapsing of the beam. Thus the idea of a mechanism was borne out.

John Gilliland

and with other relevant areas of research. The paper concludes with some basic recommendations for future research.

The paper is organized as follows. Section 2 discusses the current state of the art in the field of energy efficiency in buildings. Section 3 highlights some recent work on energy efficiency in buildings, while Section 4 provides a brief review of the literature on energy efficiency in buildings. Section 5 presents a critical review of the literature on energy efficiency in buildings, and Section 6 concludes with some final remarks.

2. THE STATE OF THE ART IN ENERGY EFFICIENCY IN BUILDINGS

There is a large literature on energy efficiency in buildings, and this section provides a brief overview of some of the key findings. The focus is on residential buildings, although some of the concepts and methods may also apply to commercial buildings. The discussion is divided into two main sections: energy efficiency in new buildings and energy efficiency in existing buildings.

2.1. Energy efficiency in new buildings

Energy efficiency in new buildings has been a major concern for many years, and there has been significant progress made in this area. One of the most important developments in this field has been the introduction of passive solar design principles, which aim to reduce the need for active heating and cooling systems by utilizing natural sunlight. This approach has been particularly effective in reducing energy consumption in new buildings, especially in warm climates where passive solar design can be used effectively.

Another important aspect of energy efficiency in new buildings is the use of high-quality insulation materials. Insulation is a key component of energy efficiency, as it helps to reduce heat loss through conduction and convection. There are several types of insulation available, including mineral wool, cellulose, and spray foam. Mineral wool is a popular choice due to its high thermal resistance and low cost. Cellulose insulation is another option, as it is made from recycled paper and is relatively inexpensive. Spray foam insulation is also a good choice, as it is highly insulating and can be applied easily to walls and roofs.

2.2. Energy efficiency in existing buildings

Energy efficiency in existing buildings is a more challenging problem than in new buildings, as it involves retrofitting existing structures to improve their energy performance. One of the main challenges in this area is the cost of retrofitting, as it can be expensive to replace old equipment and fixtures. Another challenge is the difficulty of assessing the potential savings from retrofits, as it is often difficult to predict the exact impact of different measures.

One way to address these challenges is through the use of energy audits. An energy audit is a process of examining a building's energy use and identifying opportunities for improvement. The audit typically involves a detailed assessment of the building's energy systems, including heating, cooling, and lighting. The results of the audit can then be used to develop a plan for energy efficiency improvements, such as upgrading insulation, replacing old equipment, or adding new equipment. These improvements can be relatively inexpensive and can have a significant impact on energy consumption.

Rigid Frame Tests #1, #2, and #3:

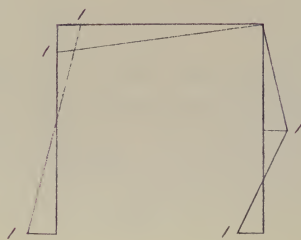
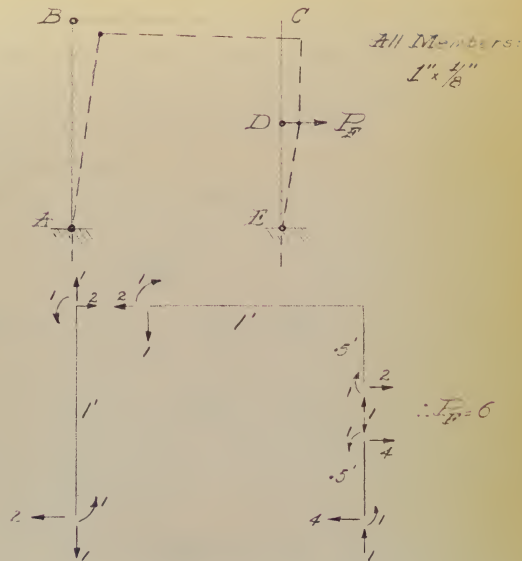
The frames used in these tests were of uniform cross section, 1" x 1/8". The legs and top member were all one foot in length. They were loaded with a concentrated load acting at the mid-point of and perpendicular to one of the legs.

As seen in Figure 10-A hinges would theoretically form at points A, B, D, and E. P_F would theoretically equal to 6. By use of the fundamental formula $M_p = 2A\bar{y}s_1$, the plastic resisting moment of the section was found to be 11.88 foot-pounds. Therefore the actual value of the failure load P would be $6 \times 11.88 = 71.3$ pounds. This follows from the fact that $P_F = 6$ was based on the existence of a unit value of plastic moment (M_p), whereas the actual value of the plastic moment equals 11.88 foot-pounds.

In all three tests (#1, #2, and #3) the first hinge formed at E; the second at D; the third at A; and the final hinge at B. The average value of the failure load as determined in the three tests was 112.2 pounds. It is to be noted that the actual value of the failure load was considerably higher than the calculated value. We attributed this to the following causes: Considerable bending took place at point E before the final hinge at B was formed. From all indications, the

FIGURE 10 A

FOR FRAME TESTS #1, #2, #3



original hinge at E passed out of the completely plastic state and the hinge tended to move away from the support and toward the load before the last hinge was formed. The following analysis is advanced to attempt to explain why the above action gave us this increased value of failure load.

Referring to Figure 10-B:

$$\text{Equation 1: } \sum M_A = 0 \quad (\text{Member AB})$$

$$.9P_1 = 2 + .436 V$$

$$\therefore V = \frac{.9P_1 - 2}{.436}$$

$$\text{Equation 2: } \sum M_B = 0 \quad (\text{Member BCD})$$

$$2 = .93V + .575 P_1$$

$$2 = .93 \left(\frac{.9P_1 - 2}{.436} \right) + .575 P_1$$

$$2 = 1.92 P_1 - 4.27 + .575 P_1$$

$$6.27 = 2.49 P_1$$

$$P_1 = 2.52$$

$$V = \frac{.9 (2.52) - 2}{.436} = .619$$

$$\text{Equation 3: } \sum M_E = 0 \quad (\text{Member ED})$$

$$2 = (.619 \times .285) + P_2 (.25)$$

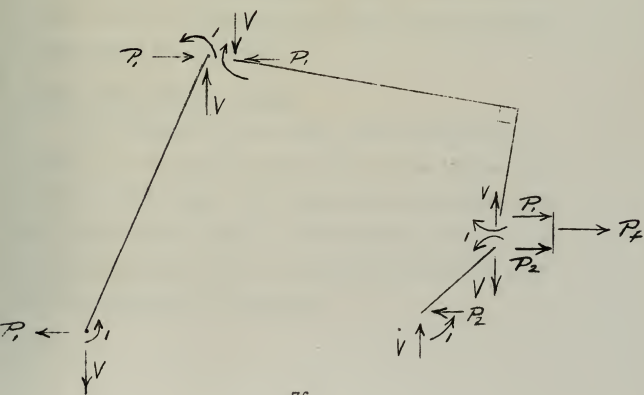
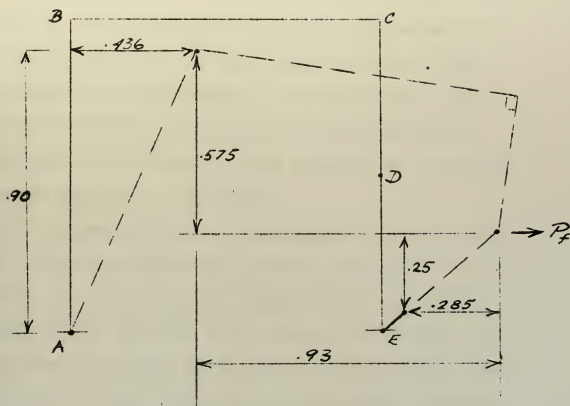
$$P_2 = 7.30$$

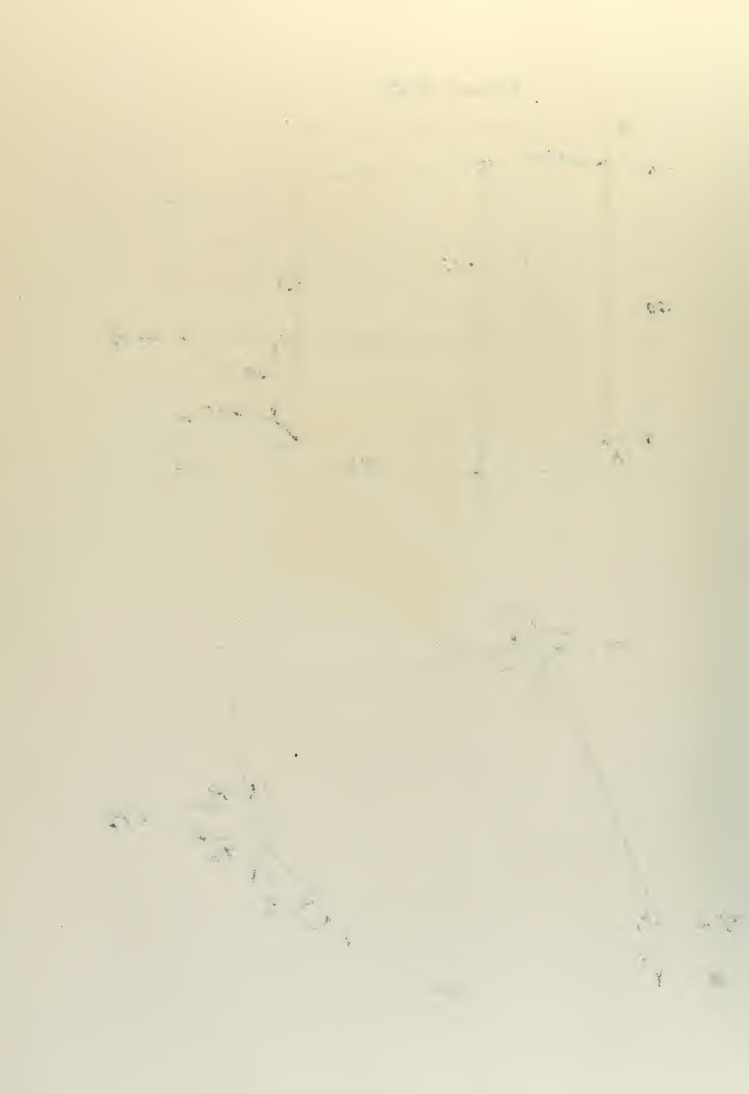
$$\text{Equation 4: } P_F = 2.52 + 7.30 = 9.82$$

$$\therefore P_F = 9.82 (11.88) = 117 \text{ lbs.}$$

Actual

FIGURE 10.3



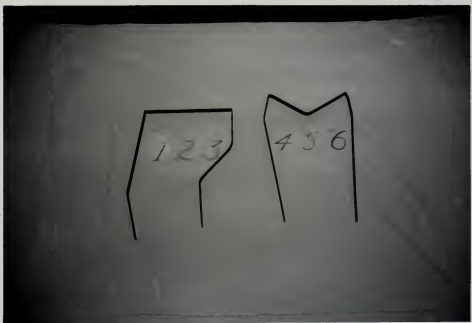


The position of the deflected frame (Figure 10-B) is not the exact configuration which existed at the time of formation of the last hinge, but is a close approximation of the actual. It accomplishes the purpose of indicating the general effect of frame distortion on the value of load required to transform the structure into a mechanism.

It is obvious that the designer is "on the safe side" if he uses for design purposes the value of P as found conventionally in Figure 10-A. If further testing proves that the actual failure load for this frame under this type of loading is always larger than the computed value, then the conventionally computed value of load might still be used for design purposes, using a safety factor smaller than is specified for other situations where computed and actual failure loads agree more closely.

Frame Tests #4, #5, and #6:

The frames used for these tests consisted of legs 1" x 1/8" strap steel with a cross member also of 1" x 1/8" stock. The legs and cross member were all one foot in length. The frame was loaded in an upright position with a concentrated vertical load at the mid-point of the span.

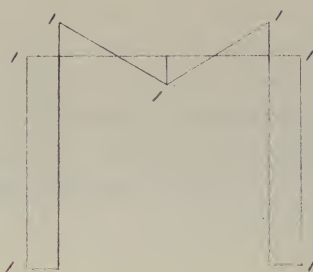
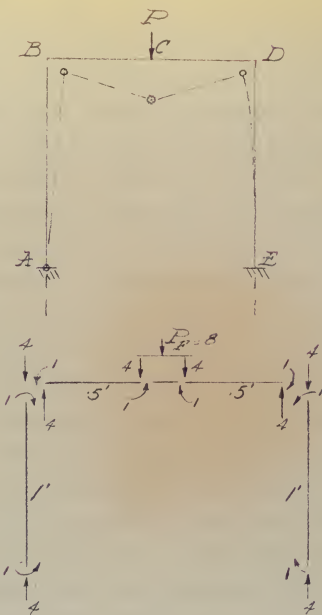


As shown in Figure 11 hinges would form at C, B, and D, and the two legs would be plastic along their entire length when the load P_F equals 8 (based on the value of the plastic moment equal to one). Since the actual value of M_p for this cross section was found to be 11.88 foot-kips, the true value of the failure load P_F equals $8 \times 11.88 = 95.0$ pounds. The value of failure load found in testing the frame was 95.6 pounds which is extremely close to the theoretical value.

The first hinge formed under the load at point C. Before the first hinged formed, each leg exhibited a point of counterflexure at a distance approximately $1/3$ of the leg height above the support. After the first hinge had formed, points B and D were free to deflect slightly inward thus causing the points of counterflexure to move downward along the leg with increasing loads. The next two hinges formed almost simultaneously at B and D. At this time, points B and D were completely free to deflect inward, thus causing the points of counterflexure to completely disappear and the two legs to become completely plastic under the action of P_F . At this time the complete structure had been transformed into a mechanism.

FIGURE 11

FOR FRAME TESTS #4, #5, #6

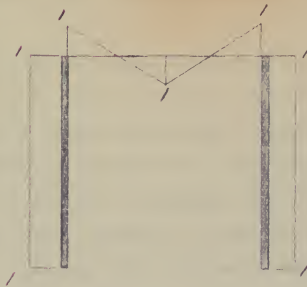
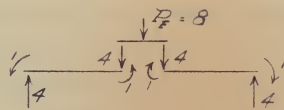
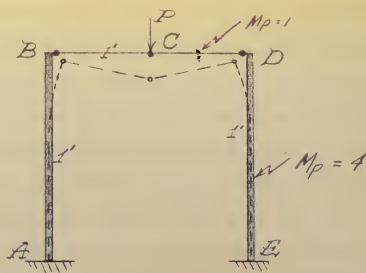


Frame Tests #7, #8, #9:

These frames had legs 1" x $\frac{1}{2}$ " and top members 1" x 1/8". All members were one foot in length. They were loaded with single concentrated loads at the mid-point of the top span. As seen in Figure 12-A, if hinges form at B, C, and D, the top span becomes a mechanism in itself and local failure occurs in the top member. In the cases represented in Figures 11 and 13, the formation of hinges at points B, C, and D made it possible for the legs of the frames to deflect inward against little restraint. The legs were essentially cantilevers loaded with a unit plastic moment and an axial force at their "free" ends. This type of loading acting on this type of structure (cantilever) would cause the plastic moment to be reached all along the legs (since M_p of legs equals one). Thus local collapse of the top members and total collapse of the structures occurred under the same load P_y .

In the case of Figure 12-A, however, a unit plastic moment and an axial force acting on top of the leg would not cause the plastic moment to be reached in the legs acting as cantilevers, since M_p of the legs equals 4. Therefore, local collapse of the top span takes place first.

FIGURE 12 A
FOR FRAME TESTS #7, #8, #9

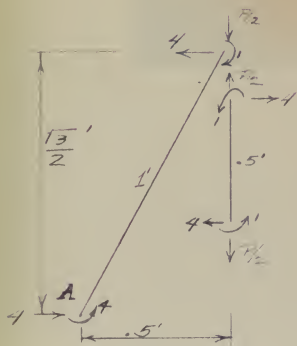
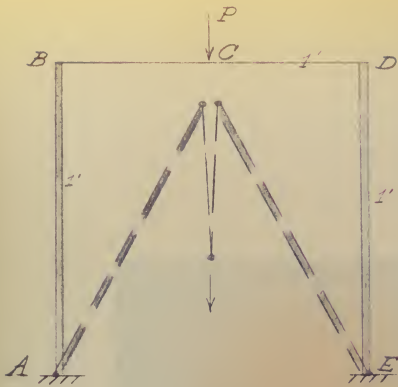


For all practical design purposes, the frame would be useless after this state of local collapse in the top member is reached. The value of load required to produce this type of collapse should therefore be considered the failure load. As seen in Figure 12-A, P_F based on a unit plastic moment equals 8. Since the plastic moment of the top member is actually 13.13, the theoretical failure load for the frame would be $8 \times 13.13 = 105.04$ pounds.

The average of the actual local failure loads in tests #7, #8, and #9 turned out to be 108.3 pounds which is in close agreement with the theoretical computed value. In loading the frame to local failure, the first plastic hinge occurred under the load at point C and the next two hinges formed simultaneously at B and D.

The problem of trying to predict the value of load which would cause the entire structure to become a mechanism is highly complicated. However, it is an easy matter to calculate the load required to bring the structure to a complete state of collapse as in Figure 12-B. However, it must be remembered that this is not the load required to transform the structure into a mechanism but is somewhat larger.

FIGURE 12 B



$$\sum M_A = 0 \\ P_B \times \frac{1}{2} = 4 - 1 + \frac{4\sqrt{3}}{2}$$

$$P = 25.8$$



We felt that it would be interesting to check our calculations as in Figure 12-B by loading to a complete state of collapse two of the frames. We predicted by our calculations that a load of 339 pounds ($25.8 \times 13.13 = 339$) would completely collapse the frames. The actual failure load turned out to be 347 pounds.

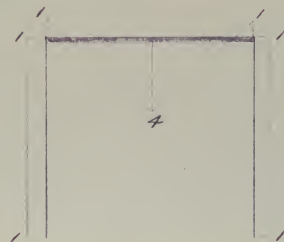
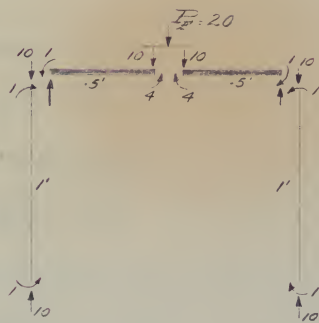
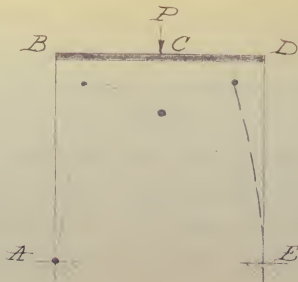
Frame Tests #10, #11, and #12:

The models used in these tests had a top member 1" x 1/4" and legs 1" x 1/8". All members were one foot in length. They were loaded with a single concentrated load at the mid-point of the top member. A theoretical analysis of the frame is shown in Figure 13-A.

Upon first looking at this frame, we felt that with a constant width, there might be some ratio of thickness of top member to leg thicknesses which would cause a simultaneous formation of hinges at points B, C, and D. The reason for thinking this was that at points B and D the hinges would form on the thinner members, the plastic moment at B and D therefore being less than at C. We believed that this smaller value of plastic moment might be reached at B and C at or before the larger value of plastic moment was reached at point C. Our analysis which

FIGURE 13 A

FOR FRAME TESTS "10," "11," "12



follows proved to us that the above could not happen, i.e., that the first hinge would always occur at C, regardless of the ratio of thicknesses of top member to legs. However, it can be seen that if the top member were made extremely thick compared with the leg, the legs would probably fail by column action before the hinge at C could form.

Referring to Figure 13-B (a), the thickness of the cross member has been termed h_c and the thickness of the legs as h_b . The width has been assumed as unity. The following ratios can be easily deduced:

Plastic Resisting Moment:

$$\frac{M_{pr-C}}{M_{pr-B}} = \frac{(h_c)^2}{(h_b)^2}$$

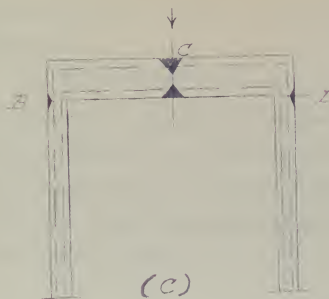
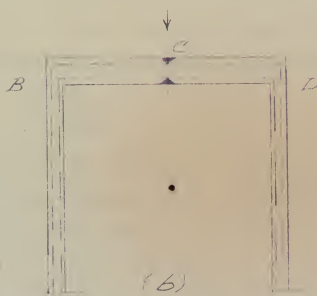
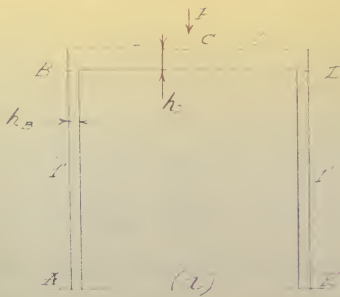
Elastic Resisting Moment:

$$\frac{M_{er-C}}{M_{er-B}} = \frac{h_c^2 \cdot f_c}{h_b^2 \cdot f_b}$$

Induced Elastic Moments Due to Load P:

$$\frac{M_{ei-C}}{M_{ei-B}} = \left(1 + \left(\frac{h_c}{h_b}\right)^3\right)$$

FIGURE 1313





It must first be proved that the yield stress at points C and B cannot be reached simultaneously:

From the above equations, if $f_c = f_b = f_y$ then,

$$(1) \frac{M_{er-C}}{M_{er-B}} = \frac{\bar{h}_c^2}{\bar{h}_b^2}$$

This equation expresses the ratio of elastic moments which must exist in order for the yield stress to be reached simultaneously at points C and B.

But the ratio of induced elastic moments equals:

$$(2) \frac{M_{ei-C}}{M_{ei-B}} = \left(1 + \left(\frac{h_c}{h_b}\right)^3\right)$$

Thus in order for the yield stress at points B and C to be reached simultaneously, Equation 1 must equal Equation 2. Therefore:

$$(3) \frac{h_c^2}{h_b^2} = \left(1 + \left(\frac{h_c}{h_b}\right)^3\right)$$

Letting the ratio of $\frac{h_c}{h_b} = K$, and substituting into Equation 3;

$$(4) K^2 = 1 + K^3$$

It can be seen that regardless of whether K equals 1; $K < 1$; or $K > 1$, there is no real solution of Equation 4. Therefore hinges can never start to form simultaneously at points C and B, and the yield stress will always be reached first at point C.

Now, referring to Figure 13-B (b), it is assumed that the yield stress has been reached first at C in the outer fibers in accordance with what we have shown above. The dotted lines indicate the elastic core remaining in the structure. The core acts in every respect like the original elastic structure; that is, the yield stress will be reached at C in the core before it will be reached at D in the core. (See Figure 13-B (c)). Therefore, this action will cause the core to disappear first at C, or in other words, the hinge forms first at C.

In Figure 13-A, hinges were assumed at points A, B, C, and D. This assumption of hinges proved to be correct. The moment diagram shows that actually the two legs are plastic throughout their length.

Assuming the conventional unit plastic moments to act at points A, B, D and E, and a relative value of plastic moment at C of $1 \times \left(\frac{1}{\frac{1}{3}}\right)^z$ or 4, then P_F equals 20.

Since the actual value of the plastic moment is 13.13 for the legs, then P_F actual equals 263 pounds.

Under loading the first hinge formed at point C under an average load of 218 pounds. Under an average failure load of 264.3 pounds hinges formed simultaneously at points B and D. At this time, points B and D deflected inward and legs AB and DE became plastic throughout their length.

Frame Test #13, #14, and #15:

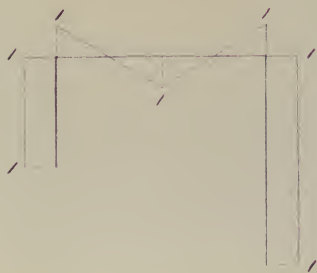
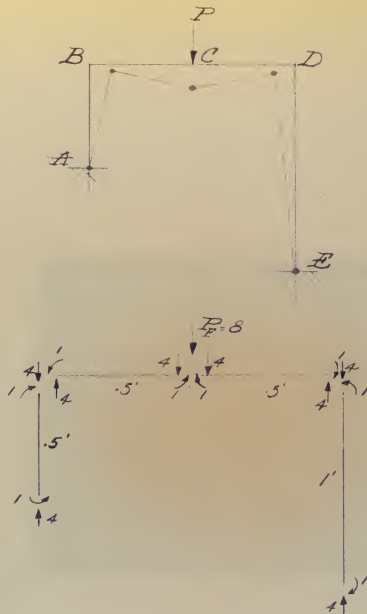
All parts of these frames were 1" x 1/8" in cross section. The span length was one foot. One leg had a length of one foot while the other leg was one-half foot in length. The frame was loaded with a vertical concentrated load at the mid-point of the top member.

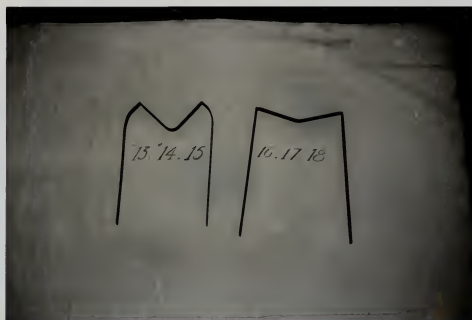
In Figure 14 our theoretical analysis is shown. Based on our previous experience, we assumed that hinges would form first at point C, then at points B and D, at which time both legs would become plastic throughout their lengths.

The theoretical value of the failure load P_f was computed to be 95.0 pounds. The actual failure load was 95.9 pounds, an average value for the three tests run.

In testing these frames side sway occurred under the lower values of loading. The first plastic hinge occurred under the load at point C. The next two occurred at points B and D simultaneously at which time both points B and D deflected inward. This action superceded the side sway in the frames. This test conformed almost exactly to our expectations based on theory. Upon hinge formation at points

FIGURE 14
FOR FRAME TESTS #13, #14, #15





B and D, the legs became plastic throughout their length with no increase in load. The photograph of the deformed structure indicates clearly that the deformed structure conformed to theoretical predictions.

Frame Tests #16, #17, and #18:

The legs of these frames were 1" x 1/4" and the top members were 1" x 1/8". The top member and one leg were one foot in length and the remaining leg was one-half in length. The frames were loaded with a concentrated vertical load at the mid-point of the top span.

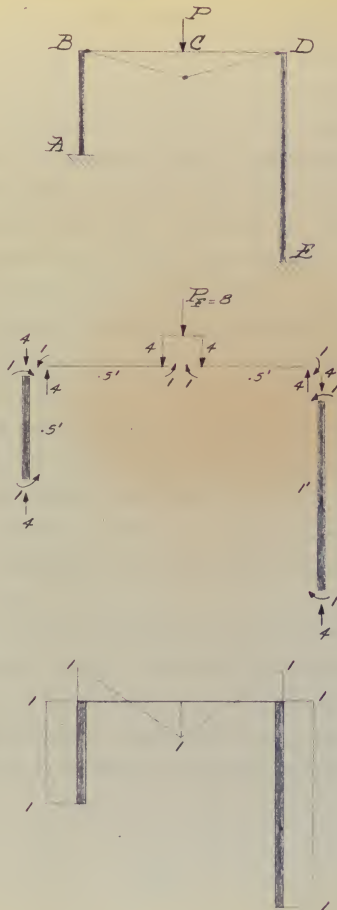
These frames were only loaded until local collapse in the top member of the frames occurred. As was pointed out in connection with Figure 12, the structure has failed for all practical purposes once local collapse has taken place. As seen in Figure 15 hinges have been assumed at points B, C, and D in the top span. This yielded a theoretical failure load of 105.04 pounds ($8 \times 13.13 = 105.04$).

The average failure load by tests #16, #17, and #18 was 106.7 pounds.

This frame behaved under loading exactly as did the frames in tests #13, #14, and #15 except that when hinges had formed at points B, C, and D, the legs AB and DE did not become plastic.

FIGURE 15

FOR FRAME TESTS #16, #17, #18



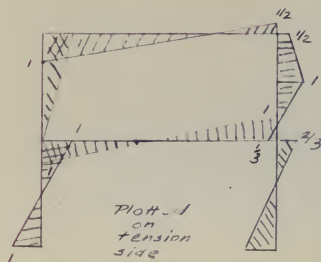
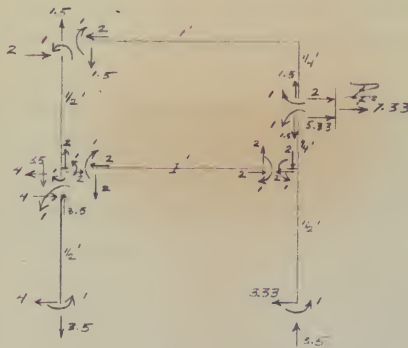
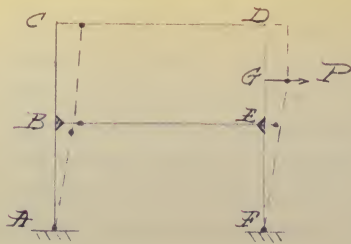
Frame Tests #19 and #20:

All parts of these frames were made 1" x 1/8". They were single bay two story frames with a span of one foot and a story height of one-half foot. The frames were formed exactly as the other frames used in our tests except that the additional cross member was welded in place. The frames were not heat treated in any way. We loaded the frames with a concentrated load acting perpendicular to the mid-point of the top story column member.

Referring to Figure 16, seven hinges have been assumed since our structure is redundant to the sixth degree ($3D + R - 3 = 3(1) + 6 - 3 = 6$). The hinges were assumed as indicated in Figure 16 from which the theoretical failure load based on a unit plastic moment was found to be 7.33. The resulting moment diagram in no place had an ordinate greater than unity, hence our hinge assumptions were correct.

The failure load based on a plastic moment of 13.13 was 96.6 pounds. The actual average failure load of tests #19 and #20 was 128.1 pounds. This obvious discrepancy between theoretical and actual failure load is probably due to the following:

FIGURE 16
FOR FRAME TESTS #19 AND #20



First of all, the material in the neighborhood of the welds has undoubtedly undergone changes in properties while being welded. Also, the welds tended to make the joints at B and E more rigid than the remaining joints in the frame due to the excess of weld material present. In addition, the reasoning advanced in frame tests #1, #2, and #3 explaining the discrepancy between actual and theoretical failure loads applied in these tests but to a lesser degree, since the overall distortion in these tests was not as great as in tests #1, #2, and #3.

The behavior of these frames under test was extremely gratifying. The hinges formed as predicted. The first hinge formed at point A, the next at F, then at nearly the same load at BE, EB, BC, and G. The last hinge formed at point C.



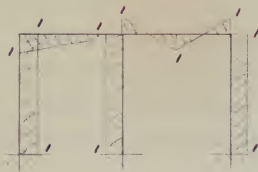
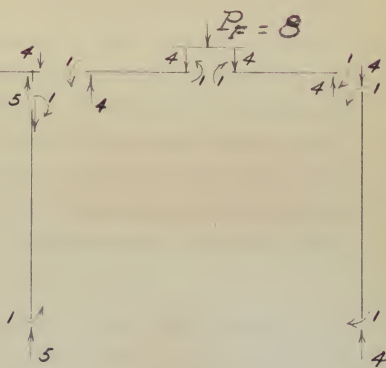
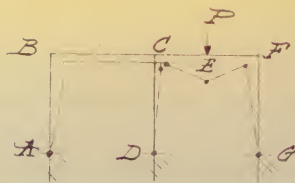
Theoretical Analysis of Two-Bay Single Story Rigid Frame:

We did not have sufficient time to construct and subject this particular frame to laboratory test. We have however undertaken the theoretical analysis of the frame. This analysis appears in Figure 17.

Seven plastic hinges are necessary to transform the structure into a mechanism. Hinges were assumed at points A, D, G, CD, CE, E, and F. Based on a unit plastic moment, our free body solution yielded a failure load of eight. Corresponding moment diagrams proved our hinge assumptions to be correct.

It is to be noted that in this frame that member CF fails locally first. Then points C and F are free to deflect inward against little restraint and legs BA, CD, and FG are free to become plastic throughout their lengths. Thus local and total collapse of the structure occurs under the same value of load. However, if legs BA, CD, and FG were thicker than the cross members the frame would fail by local collapse in member CF.

FIGURE 17



CONCLUSIONS

From our investigations we have formed the following opinions:

(1) We believe that the procedure we have outlined for the analysis of simple rigid frames is both valid and practical. In all cases we found that hinges occurred exactly where we predicted they would. The actual value of the failure load found by experimentation was never smaller than our computed value. It appears that most of the factors introducing discrepancies between theoretical and actual behavior placed the theoretical computations on the safe side.

(2) We believe that the LIMIT design of structures is of great value in that it gives the designer a true picture of the strength of the structure, which certainly should be of primary concern. We believe that after some study is given the problem, a suitable safety factor could be introduced into the limit design of the structure such that under maximum actual loading conditions the structure would have no more than the first

plastic hinge formed. From our observations of deflected structures, the deflections occurring upon formation of the first plastic hinge were of the order of elastic deflections. They were perhaps slightly larger than would be allowed by present codes, but we feel that these allowed deflections could and should be increased in most cases. At any rate, the whole problem should be given increased thought. With the decrease of the steel supply in this country, limit design procedures provide a tool with which maximum economy can be introduced into the design of structures of all types.

RECOMMENDATIONS

We suggest the following to future investigators undertaking similar work in the field of limit design:

- (a) The loading machine developed in the Structures Department might be used to advantage since, with it, it is possible to use multiple loads on various test structures.
- (b) Heat treat structures particularly if any welding is used in their fabrication.
- (c) Use SR-type electrical strain gages at points of expected plastic hinges to determine more accurately the time of exact formation of the hinges. We feel that this would be the most direct way to determine hinge formations.
- (d) The recommendations of Butler and Gibson in their thesis as to future work which should be undertaken in continuing the work already started cover the possibilities.

APPENDIX

Frame Test # 1:

<u>Load Added</u>	<u>Accumulated Weight</u>	<u>Deflection at Load Point in Inches</u>
0.00	0.00	0
2.60	2.60	.012
6.95	9.55	.043
7.75	17.30	.108
7.50	24.80	.157
8.45	33.25	.215
8.30	41.55	.275
8.15	49.70*	.397
5.70	55.40	.488
6.50	61.90	
7.50	69.40	
4.00	73.40**	Deflection dial observed after this point.
3.60	77.00***	
2.00	79.00	Deflections were not recorded.
3.10	82.10	
7.20	89.30	
3.20	92.50	
4.00	96.50	
2.00	98.50	
2.00	100.50	
2.00	102.50	
2.00	104.50	
2.00	106.50	
2.00	108.50	
2.00	110.50	
2.00	112.50****	

* First hinge formed at point E.

** Second hinge formed at point D.

*** Third hinge formed at point A.

**** Fourth hinge formed at point B.

Frame Test # 2:

<u>Load Added</u>	<u>Accumulated Weight</u>	<u>Deflection at Load Point in Inches</u>
0.00	0.00	0
2.60	2.60	.015
7.50	10.10	.077
8.15	18.25	.146
6.95	25.20	.168
7.75	32.95	.218
8.45	41.40	.276
8.30	49.70**	.408
7.75	57.45	.506
8.15	65.60	
5.70	71.30***	
8.00	79.30***	Deflection dial observed after this point.
6.40	85.70	
3.10	88.80	
4.00	92.80	Deflections were not recorded.
2.00	94.80	
2.00	96.80	
2.00	98.80	
2.00	100.80	
2.00	102.80	
2.00	104.80	
2.00	106.80	
2.00	108.80	
2.00	110.80	
.40	111.20	
.40	111.60	
.40	112.00	
.40	112.40	
.40	112.80	
.40	113.20	
.40	113.60****	

* First hinge formed at point E.

** Second hinge formed at point D.

*** Third hinge formed at point A.

**** Fourth hinge formed at point B.

1994

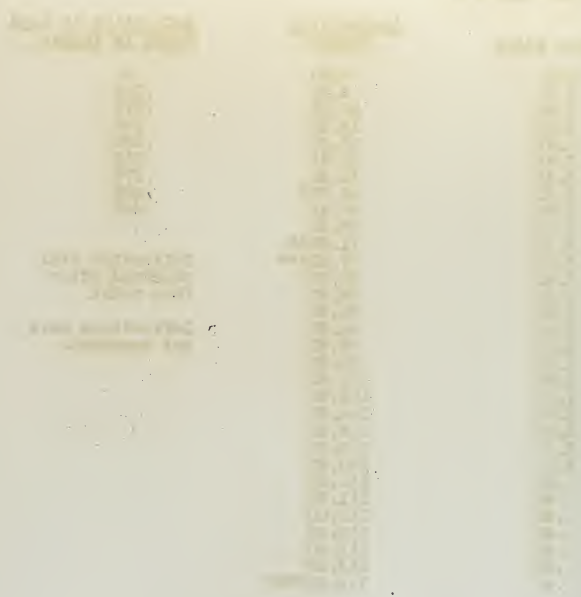


Fig. 1. Vertical blocks used in traditional building techniques. (a) Vertical blocks used in traditional building techniques; (b) vertical blocks used in traditional building techniques.

the vertical blocks were joined together by a horizontal binding system.

The vertical blocks were made from a single piece of wood or bamboo.

The vertical blocks were made from a single piece of wood or bamboo.

The vertical blocks were made from a single piece of wood or bamboo.

The vertical blocks were made from a single piece of wood or bamboo.

The vertical blocks were made from a single piece of wood or bamboo.

The vertical blocks were made from a single piece of wood or bamboo.

Frame Test # 3:

<u>Load Added</u>	<u>Accumulated Weight</u>	<u>Deflection at Load Point in Inches</u>
0.00	0.00	0.00
2.60	2.60	0.014
6.95	9.55	0.046
7.50	17.05	0.112
8.45	25.50	0.166
8.30	33.80	0.221
7.75	41.55	0.276
7.20	48.75	0.371
0.80	49.55	0.391
0.40	49.95	0.401
0.40	50.35*	0.407
5.50	56.85	0.501
7.30	64.15	
8.30	72.45	
0.80	73.25	
0.40	73.65	Deflection dial observed after this point.
0.40	74.05**	
1.60	75.65	
1.60	77.25	
0.40	77.65***	Deflections were not recorded.
7.70	85.35	
7.60	92.95	
6.70	99.65	
4.00	103.65	
1.60	105.25	
1.20	106.45	
2.00	108.45	
2.00	110.45****	

* First hinge formed at point E.

** Second hinge formed at point D.

*** Third hinge formed at point A.

**** Fourth hinge formed at point B.

Frame Test # 4:

<u>Load Added</u>	<u>Accumulated Weight</u>	<u>Deflection at Load Point in Inches</u>
0.00	0.00	0.000
34.60	34.60	0.138
25.00	59.60*	0.249
25.00	84.60	
5.70	90.30	Deflection dial observed after this point.
1.60	91.90	
1.30	93.50	
1.60	95.10	Deflections were
0.40	95.60**	not recorded.

* Hinge formed under load at point C.

** Hinges at points B and D and multi-hinges in legs.

Frame Test # 5:

<u>Load Added</u>	<u>Accumulated Weight</u>	<u>Deflection at Load Point in Inches</u>
0.00	0.00	0.000
34.60	34.60	0.142
25.00	59.60	0.251
1.20	60.80*	
25.00	85.80	Deflection dial observed after this point.
7.20	93.00	
2.00	95.00	
2.00	97.00**	Deflections were not recorded.

* Hinge formed under load at point C.

** Hinges at points B and D and multi-hinges in legs.

Frame Test # 6:

<u>Load Added</u>	<u>Accumulated Weight</u>	<u>Deflection at Load Point in Inches</u>
0.00	0.00	
34.60	34.60	
8.30	42.90	
8.40	51.30	
4.00	55.30	
2.80	58.10	
0.80	58.90*	
25.00	83.90	
2.40	86.30	
2.00	88.30	
2.00	90.30	
2.00	92.30	
2.00	94.30**	

* Hinge formed under load at point C.

** Hinges at points B and D and multi-hinges in legs.

Frame Test # 7:

<u>Load Added</u>	<u>Accumulated Weight</u>	<u>Deflection at Load Point in Inches</u>
0.00	0.00	0.000
34.00	34.00	0.074
25.00	59.00	0.133
25.00	84.00	0.189
6.95	90.95	0.204
8.00	98.95*	0.301
2.00	100.95	
2.00	102.95	Deflection dial observed after this point.
2.00	104.95	
.40	105.35	
.40	105.75	Deflections were not recorded.
.40	106.15**	
.40	106.55	
.40	106.95	
.40	107.35	
.40	107.75***	

* Hinge formed under load at point C.

** Hinge formed at point B on thin member BC.

*** Hinge formed at point D on thin member DC.

Frame Test # 8:

<u>Load Added</u>	<u>Accumulated Weight</u>	<u>Deflection at Load Point in Inches</u>
0.00	0.00	0.000
34.00	34.00	0.069
25.00	59.00	0.131
25.00	84.00	0.186
6.95	90.95	0.213
2.00	92.95	0.229
2.00	94.95	0.240
2.00	96.95	0.257
0.80	97.75	0.268
0.40	98.15	0.274
0.40	98.55	0.281
0.40	98.95	0.287
0.40	99.35	0.301
0.40	99.75*	0.320
2.00	101.75	
2.00	103.75	Deflection dial observed after this point.
2.00	105.75	
.80	106.55**	
.80	107.35	Deflections were not recorded.
.80	108.15***	

* Hinge formed under load at point C.

** Hinge formed at point D in thin member DC.

*** Hinge formed at point E in thin member BC.

Frame Test # 9:

<u>Load Added</u>	<u>Accumulated Weight</u>	<u>Deflection at Load Point in Inches</u>
0.00	0.00	0.000
34.00	34.00	0.073
25.00	59.00	0.136
25.00	84.00	0.191
8.00	92.00	0.234
6.70	98.70*	0.306
8.30	107.00	Deflection dial observed after this point.
.80	107.80	
.80	108.60	
.40	109.00**	Deflections were not recorded.

* Hinge formed under load at point C.

** Hinges formed simultaneously at points B and D on thin members BC and DC.

Frame Test # 10:

<u>Load Added</u>	<u>Accumulated Weight</u>	<u>Deflection at Load Point in Inches</u>
0.00	0.00	0.000
34.00	34.00	0.030
25.00	59.00	0.047
25.00	84.00	0.070
25.00	109.00	0.086
25.00	134.00	0.110
25.00	159.00	0.131
25.00	184.00	0.153
25.00	209.00	0.171
8.50	217.30*	0.292
7.80	225.10	Deflection dial observed after this point.
8.10	233.20	
8.40	241.60	
8.15	249.75	
8.10	257.85	Deflections were not recorded.
8.40	266.25**	

* Hinge formed under load at point C.

** Hinges formed at points B and D.

Legs AB and DE became plastic throughout their lengths.

Frame Test # 11:

<u>Load Added</u>	<u>Accumulated Weight</u>	<u>Deflection at Load Point in Inches</u>
0.00	0.00	0.000
34.00	34.00	0.037
25.00	59.00	0.051
25.00	84.00	0.076
25.00	109.00	0.091
25.00	134.00	0.117
25.00	159.00	0.134
25.00	184.00	0.156
25.00	209.00	0.177
7.60	216.60*	0.311
7.80	224.40	
8.10	232.50	Deflection dial observed after
8.30	240.80	this point.
8.40	249.20	
8.00	257.20	Deflections were
6.70	263.90**	not recorded.

* First hinge formed under load at point C.

** Hinges formed at points B and D.

Legs AB and DE became plastic throughout their lengths.

Frame Test # 12:

<u>Load Added</u>	<u>Accumulated Weight</u>	<u>Deflection at Load Point in Inches</u>
0.00	0.00	0.000
34.00	34.00	0.032
25.00	59.00	0.049
25.00	84.00	0.076
25.00	109.00	0.090
25.00	134.00	0.117
25.00	159.00	0.135
25.00	184.00	0.155
25.00	209.00	0.178
8.10	217.10	0.201
2.00	219.10	0.217
2.00	221.10*	0.307
8.30	229.4	
8.40	237.8	Deflection dial observed after this point.
7.80	245.6	
8.30	253.9	
6.80	260.7	Deflections were
2.00	262.7**	not recorded.

* First hinge formed under load at point C.

** Hinges formed at points B and D.

Legs AB and DE became plastic throughout their length.

Frame Test # 13:

<u>Load Added</u>	<u>Accumulated Weight</u>	<u>Deflection at Load Point in Inches</u>
0.00	0.00	0.000
9.00	9.00	0.031
25.00	34.00	0.131
25.00	59.00	0.269
8.70	67.70	0.327
7.30	75.00*	0.560
8.70	83.70	
8.10	91.80	Deflection dial observed after this point.
2.00	93.80	
1.20	95.00**	
.40	95.40***	Deflections were not recorded.

* First hinge formed under load at point C.

** Second hinge formed at point B.

*** Third hinge formed at point D.

Frame Test # 14:

<u>Load Added</u>	<u>Accumulated Weight</u>	<u>Deflection at Load Point in Inches</u>
0.00	0.00	0.000
9.00	9.00	0.037
25.00	34.00	0.139
25.00	59.00	0.269
8.70	67.70	0.319
7.30	75.00	0.427
.40	75.40*	0.547
8.70	84.10	
8.10	92.20	Deflection dial observed after this point.
2.00	94.20	
1.20	95.40**	
.40	95.80	
.40	96.20***	Deflections were not recorded.

* First hinge formed under load at point C.

** Second hinge formed at point D.

*** Third hinge formed at point B.

Frame Test # 15:

<u>Load Added</u>	<u>Accumulated Weight</u>	<u>Deflection at Load Point in Inches</u>
0.00	0.00	0.000
9.00	9.00	0.031
25.00	34.00	0.138
25.00	59.00	0.271
8.70	67.70	0.321
7.00	74.70	0.420
0.40	75.10*	0.542
8.70	83.80	
8.10	91.90	Deflection dial observed after this point.
2.00	93.90	
1.20	95.10**	
0.80	95.90***	Deflections were not recorded.

* First hinge formed under load at point C.

** Second hinge formed at point B.

*** Third hinge formed at point D.

Frame Test # 16:

<u>Load Added</u>	<u>Accumulated Weight</u>	<u>Deflection at Load Point in Inches</u>
0.00	0.00	0.000
9.00	9.00	0.049
25.00	34.00	0.108
25.00	59.00	0.179
25.00	84.00	0.250
8.30	92.30	0.320
4.00	96.30*	0.440
4.00	100.30	
2.00	102.30	Deflection dial observed after this point.
2.00	104.30**	
2.00	106.30***	Deflections were not recorded.

* First hinge formed under load at point C.

** Second hinge formed at point BC.

*** Third hinge formed at point DC.

Frame Test # 17:

<u>Load Added</u>	<u>Accumulated Weight</u>	<u>Deflection at Load Point in Inches</u>
0.00	0.00	0.000
9.00	9.00	0.047
25.00	34.00	0.110
25.00	59.00	0.181
25.00	84.00	0.249
8.30	92.30	0.326
2.00	94.30	0.331
0.80	95.10	0.352
0.80	95.90	0.367
0.40	96.30*	0.432
4.00	100.30	
2.00	102.30	Deflection dial observed after this point.
2.00	104.30**	
0.80	105.10	
0.40	105.50	Deflections were not recorded.
0.40	105.90	
0.40	106.30	
0.40	106.70***	

* First hinge formed under load at point C.

** Second hinge formed at point DC.

*** Third hinge formed at point BC.

Frame Test # 18:

<u>Load Added</u>	<u>Accumulated Weight</u>	<u>Deflection at Load Point in Inches</u>
0.00	0.00	0.000
9.00	9.00	0.043
25.00	34.00	0.105
25.00	59.00	0.177
25.00	84.00	0.239
8.30	92.30	0.319
2.00	94.30	0.351
2.00	96.30	0.387
0.80	97.10*	0.451
2.00	99.10	
4.00	103.10	Deflection dial
2.00	105.10**	observed after
2.00	107.10***	this point.
		Deflections were not recorded.

* First hinge formed under load at point C.

** Second hinge formed at point BC.

*** Third hinge formed at point DC.

Frame Test # 19:

<u>Load Added</u>	<u>Accumulated Weight</u>	<u>Deflection at Load Point in Inches</u>
0.00	0.00	
6.00	6.00	
8.45	14.45	
7.15	21.60	
8.00	29.60	
7.20	36.80	
8.15	44.95	
7.65	52.60	
8.30	60.90	
6.10	67.00	
5.70*	72.70	
8.30	81.00	
8.40	89.40	
6.10**	95.50	
4.00***	99.50	
2.00****	101.50	
8.70	110.20	
4.00	114.20	
4.00	118.20	
4.00	122.20	
1.20	123.40	
1.20	124.60	
1.20	125.80	
1.20	127.00	
1.20*****	128.20	

* First hinge formed at point A.

** Second hinge formed at point F.

*** Third hinge formed at points BE and EB.

**** Fourth hinge formed at points BC and G.

***** Fifth hinge formed at point C.

Frame Test # 20:

<u>Load Added</u>	<u>Accumulated Weight</u>	<u>Deflection at Load Point in Inches</u>
0.00	0.00	
6.00	6.00	
8.45	14.45	
7.15	21.60	
8.00	29.60	
7.20	36.80	
8.15	44.95	
7.65	52.60	
8.30	60.90	
6.10	67.00	
1.20	68.20	
1.20	69.40	
2.00*	71.40	
8.30	79.70	
8.40	88.10	
2.00	90.10	
2.00	92.10	
2.00	94.10	
1.20**	95.30	
2.00	97.30	
2.00***	99.30	
2.00	101.30	
0.40****	101.70	
8.70	110.40	
4.00	114.40	
8.00	122.40	
4.00	126.40	
1.20	127.60	
0.40*****	128.00	

* First hinge formed at point A.

** Second hinge formed at point F.

*** Third hinge formed at points BE and EB.

**** Fourth hinge formed at points BC and G.

***** Fifth hinge formed at point C.

Thesis 15637
M67 Monaghan
An investigation of
the formation of plastic
hinges in simple rigid
frames.

Thesis 15637
M67 Monaghan
An investigation of
the formation of plastic
hinges in simple rigid
frames.

thesM67
An investigation of the formation of pla



3 2768 002 04693 0
DUDLEY KNOX LIBRARY